Engineering Journal of Qatar University, Vol.6, 1993, p. 157-176

THE ONSET OF RESONANCE IN TWO-IMMISCIBLE FLUIDS INSIDE A SPINNING AND CONING CYLINDER

M. Selmi
Department of Mechanical Engineering
Qatar University, Doha, Qatar.

ABSTRACT

Resonance of the motion of two fluids inside a cylinder that spins about its axis and rotates (cones) about an axis that passes through its center of mass is known to occur for low-viscosity fluids (high Reynolds number flows) at critical geometric parameters and coning frequencies. In this paper the motion of two inviscid fluids inside a spinning and coning cylinder is analyzed by the method of separation of variables for small coning frequencies and/or coning angles. The analytical solution of the inviscid flow equations provides a criterion in the form of a transcendental equation that governs the behavior of the parameters that cause resonance. The transcendental equation was solved numerically by Newton-Raphson's iteration and the results are in good agreement with those obtained for two viscous fluids.

INTRODUCTION

Spin-stabilized liquid-filled projectiles are known to experience severe dynamical instabilities owing to the motion of their liquid payload. For cylinders completely filled with a single fluid we know two types of instabilities that are excited by the coning motion of the projectile about its flight trajectory.

One of the instabilities is caused by resonance with inertial waves at critical coning frequencies (ratio of the coning rate Ω to the spin rate ω) and is most pronounced for fluids of low viscosity, i.e. high Reynolds numbers. We define the Reynolds number as $\mathrm{Re}=\omega a^2/\nu$, where a is the radius of the cylinder and ν is the kinematic viscosity of the liquid. This instability is

known to strongly depend on the cylinder aspect ratio (ratio of the length $2c$ of the cylinder to its diameter $2a$). For stable designs, the aspect ratio is properly chosen to avoid resonance for a given coning frequency. The Stewartson-Wedemeyer theory is appropriate for this task. While Stewartson (1959) has solved for the critical coning frequencies, Wedemeyer (1966) has added the boundary layer theory to actually estimate the moments exerted by the fluid inside the cylinder.

The other instability is due to viscous stresses applied on the walls of the payload container and is most pronounced for fluids of high viscosity, i.e. low to medium Reynolds numbers, for a wide range of aspect ratios and coning frequencies. The moments exerted by the fluid inside the cylinder can be calculated by the methods of Herbert & Li (1990), Hall *et al.* (1990), and Selmi *et al.* (1992). Accurate calculations of the moments are needed for flight simulation at a wide range of Reynolds number.

While the instability due to resonance with inertial waves is easily avoided by proper design, the viscous instability is hard to eliminate. It was suggested (Miller 1991) that a low-viscosity additive might lessen the viscous stresses applied on the walls of the cylinder. To find out if this is the case, the motion of two immiscible viscous fluids has been analyzed by Selmi and Herbert (see Selmi (1991) and Selmi *et al.* (1993)). While it was discovered that a low viscosity additive can eliminate the viscous instability under certain conditions, it was found out that under other conditions the motion is susceptible to resonance. For a core fluid that is very viscous and additive that is low in viscosity, resonance can occur at very low density ratios. We define the density ratio as the ratio of the density of the core fluid to the density of the additive. Resonance in this case is similar to that in partially filled cylinders and has been analyzed by Selmi & Herbert (1992). For two low-viscosity fluids resonance, can occur at a wide range of parameters and this paper is concerned with the finding of these parameters.

GOVERNING EQUATIONS

We consider the steady flow of two immiscible-inviscid fluids of different densities inside a cylinder of radius a and length $2c$. The cylinder is rotating about its axis at the spin rate ω and rotating about an axis that passes through its center of mass at the coning rate Ω, and is completely filled with both fluids at a specific fill ratio. We define the fill ratio as the ratio of the volume of the heavier fluid V_1 to the total volume of the cylinder V. Under

the influence of centrifugal forces the heavy fluid, having density ρ_1, accumulates at the side walls while the lighter fluid, having density $\rho_0 < \rho_1$, surrounds the cylinder axis. The shape of the interface of the two fluids when the cylinder is spinning about its axis is an axisymmetric surface of radius a_0. This radius is an alternative measure to the fill ratio and we will refer to it as the fill radius. When the cylinder spins and cones simultaneously, the fill radius is no longer constant, but varies with the axial and azimuthal directions, and we denote this quantity by a_f. When the spin rate ω is much larger than the coning rate Ω, as in practical applications (Miller 1991), the deviation of a_f from a_0 is small. In this paper it is assumed that this is the case.

For convenience, we adopt the notion of an inner region (characterized by the index 0) that contains the inner fluid and an outer region (characterized by the index 1) that contains the outer fluid. We use Cartesian coordinates x, y, z, where z is the spin axis and x is normal to z and coplanar with both the spin axis and the coning axis Z. The angle between spin axis and coning axis is denoted by θ as shown in figure 1. When written with respect to the coning system (x, y, z), that rotates about the Z-axis of the inertial system (X, Y, Z) at the coning rate Ω, the governing equations take the form

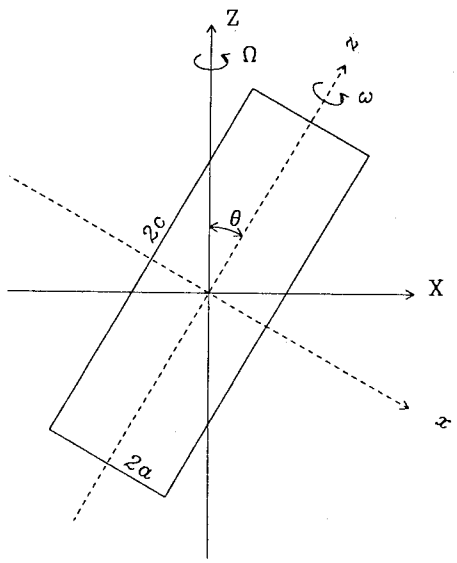

Figure 1: Description of geometry

$$\nabla \cdot \mathbf{V} = 0, \tag{1a}$$

$$\rho \left[\frac{D}{Dt}(\mathbf{V}) + 2\Omega \mathbf{k} \times \mathbf{V} + \Omega \mathbf{k} \times (\Omega \mathbf{k} \times \mathbf{r}) \right] = -\nabla P, \tag{1b}$$

where $\mathbf{V}$ and P denote the velocity and pressure respectively, ρ is the density, $\mathbf{k}$ is a unit vector in the Z direction, and $\mathbf{r}$ is the position vector. The density ρ takes the value ρ_0 when in the inner region and the value ρ_1 when in the outer region.

The flow quantities are made dimensionless by using ρ to scale mass, a to scale length, and ω to scale time. Hence from here on all quantities are dimensionless and the problem depends on the aspect ratio $\eta = a/c$, the coning frequency $\tau = \Omega/\omega$, the coning angle θ, the dimensionless fill radius $r_0 = a_0/a$ (or the fill ratio $f = V_1/V$), and the density ratio ρ_0/ρ_1. For convenience, the flow variables are expressed in cylindrical coordinates (r,ϕ,z), where r is in the radial direction, ϕ is in the azimuthal direction, and z is along the axis of the cylinder. Also for convenience, the velocity and pressure are split according to

$$\mathbf{V} = \mathbf{v}^s + \mathbf{v}, \; P = -\tfrac{1}{2}(1+\tau_z)^2 r_0^2 + p^s + p^d, \tag{2}$$

where $\mathbf{v}^S$ is the velocity due to solid body rotation, $\tau_Z = \tau \cos\theta$, and p^S is chosen so that the forcing terms in the governing equations reduce to only one term present in the z-momentum equation,

$$p^s = \tfrac{1}{2}\left[r^2(1+\tau_z)^2 + r^2\tau_\phi^2 + z^2\varepsilon^2 - 2rz\tau_z\tau_r \right], \tag{3}$$

where $\tau_r = -\varepsilon \cos\phi$, $\tau_\phi = \varepsilon \sin\phi$, and $\varepsilon = \tau \sin\theta$. We represent the velocity deviation from solid-body rotation by

$$\mathbf{v} = (v_r, v_\phi, v_z) = \begin{cases} \mathbf{v}_0 = (v_r^0, v_\phi^0, v_z^0) \text{ if } 0 \le r \le r_f, \\ \mathbf{v}_1 = (v_r^1, v_\phi^1, v_z^1) \text{ if } r_f \le r \le 1, \end{cases} \tag{4a}$$

the perturbation pressure by

$$p^d = \begin{cases} p_0^d \text{ if } 0 \le r \le r_f, \\ p_1^d \text{ if } r_f \le r \le 1, \end{cases} \tag{4b}$$

and the density by

$$\rho = \begin{cases} \rho_0 \text{ if } 0 \le r \le r_f, \\ \rho_1 \text{ if } r_f \le r \le 1, \end{cases} \tag{5}$$

where

$$r_f = \frac{a_f}{a} = r_0 + \zeta(\phi, z) \tag{6}$$

is the dimensionless radial distance from the center of the cylinder to the interface and ζ is the deviation of r_f from r_0.

The equations governing the velocity components v_r, v_ϕ, v_z and the perturbation pressure p^d take the form

$$\frac{1}{r}\frac{\partial}{\partial r}(rv_r) + \frac{1}{r}\frac{\partial v_\phi}{\partial \phi} + \frac{\partial v_z}{\partial z} = 0, \tag{7a}$$

$$D' v_r - \frac{v_\phi^2}{r} - 2(1+\tau_z)v_\phi + 2\tau_\phi v_z = -\frac{\partial p^d}{\partial r}, \tag{7b}$$

$$D' v_\phi + \frac{v_r v_\phi}{r} + 2(1+\tau_z)v_r - 2\tau_r v_z = -\frac{1}{r}\frac{\partial p^d}{\partial \phi}, \tag{7c}$$

$$D' v_z + 2\tau_r v_\phi - 2\tau_\phi v_r = -\frac{\partial p^d}{\partial z} - 2r\tau_r, \tag{7d}$$

where

$$D' = \frac{\partial}{\partial t} + \frac{\partial}{\partial \phi} + v_r\frac{\partial}{\partial r} + \frac{v_\phi}{r}\frac{\partial}{\partial \phi} + v_z\frac{\partial}{\partial z}.$$

These equations are supplemented by the no-penetration conditions at the end walls ($z = \pm\eta$) and at the side wall ($r = 1$),

$$v_z^0 = v_z^1 = 0 \text{ at } z = \pm\eta, \tag{8a}$$

$$v_r^1 = 0 \text{ at } r = 1. \tag{8b}$$

They are also supplemented with the condition of continuity of normal stress (pressure) across the interface. For small interface deviation from the

axisymmetric surface $r = r_0$, this condition is applied at $r = r_0$ and takes the form

$$\rho_0\left[-p_0^{\mathrm{d}} - \tfrac{1}{2}\left\{(2r_0\zeta)(1+\tau_z)^2 + 2r_0 z\tau_z\varepsilon\cos\phi\right\}\right]$$
$$= \rho_1\left[-p_1^{\mathrm{d}} - \tfrac{1}{2}\left\{(2r_0\zeta)(1+\tau_z)^2 + 2r_0 z\tau_z\varepsilon\cos\phi\right\}\right], \qquad (9a)$$

and from kinematics, we have

$$v_{\mathrm{r}}^0 = v_{\mathrm{r}}^1 = \frac{\partial\zeta}{\partial\phi} \text{ at } r = r_0. \qquad (9b)$$

Equations (9a) and (9b) are combined to eliminate ζ from the interface condition (9a),

$$\left\{\begin{array}{l}\rho_0[-\dfrac{\partial p_0^{\mathrm{d}}}{\partial\phi} - r_0 v_{\mathrm{r}}^0(1+\tau_z)^2] - \\ \rho_1[-\dfrac{\partial p_1^{\mathrm{d}}}{\partial\phi} - r_0 v_{\mathrm{r}}^1(1+\tau_z)^2]\end{array}\right\} = -(\rho_0 - \rho_1)r_0 z\tau_z\varepsilon\sin\phi. \qquad (9c)$$

The only forcing of the flow quantities comes from the term $-2r\tau_{\mathrm{r}} = 2\varepsilon r\cos\phi$ in the z-momentum equation and the term $-(\rho_0 - \rho_1)r_0 z\tau_z\varepsilon\sin\phi$ present in boundary condition (9c). When these terms vanish, $\varepsilon = 0$, the governing equations admit the trivial solution $\mathbf{v} \equiv 0$, $p^{\mathrm{d}} \equiv 0$, and $\zeta \equiv 0$. Hence, the velocity deviation from solid body rotation and the deviation of the two-fluid interface from that corresponding to pure spinning are $O(\varepsilon)$. Moreover, if $(v_{\mathrm{r}}, v_\phi, v_z, p^{\mathrm{d}}, \zeta)$ is the solution at (r,ϕ,z), the solution at $(r,\phi+\pi,-z)$ is $(v_{\mathrm{r}}, v_\phi, -v_z, p^{\mathrm{d}}, \zeta)$.

In practical applications (Miller 1991), the parameter ε is small, i.e. $\varepsilon \le 0.05$ for $\theta \le 20°$, $\Omega \le 500$ rpm, and $\omega \ge 3000$ rpm. Since the flow quantities are $O(\varepsilon)$, then for sufficiently small ε, it is well justified (Herbert 1985) to use ε to linearize the governing equations. When this is

done, the continuity equation remains unchanged while the momentum equations for steady state conditions are written as

$$\frac{\partial v_r}{\partial \phi} - 2(1+\tau_z)v_\phi = -\frac{\partial p^d}{\partial r}, \tag{10a}$$

$$\frac{\partial v_\phi}{\partial \phi} + 2(1+\tau_z)v_r = -\frac{1}{r}\frac{\partial p^d}{\partial \phi}, \tag{10b}$$

$$\frac{\partial v_z}{\partial \phi} = -\frac{\partial p^d}{\partial z} - 2r\tau_r. \tag{10c}$$

These equations support the additional symmetries: $\mathbf{v}(r,\phi+\pi,z) = -\mathbf{v}(r,\phi,z)$, $p^d(r,\phi+\pi,z) = -p^d(r,\phi,z)$, and $\zeta(\phi+\pi,z) = -\zeta(\phi,z)$.

SOLUTION PROCEDURE

We represent the velocity field by the Fourier series

$$\mathbf{v}_\alpha(r,\phi,z) = \sum_{n=-\infty}^{\infty} \mathbf{v}_\alpha^n(r,z)e^{in\phi}, \qquad \mathbf{v}_\alpha^n = (u_\alpha^n, v_\alpha^n, w_\alpha^n), \tag{11a}$$

where α takes the value of 0 or 1 and $i^2 = -1$. Similarly we represent the interface deviation from the surface $r = r_0$ by

$$\zeta(\phi,z) = \varepsilon \sum_{n=-\infty}^{\infty} \zeta_n(z)e^{in\phi}, \tag{11b}$$

and the perturbation pressure by

$$p_\alpha^d(r,\phi,z) = 2r\varepsilon z\cos\phi + \sum_{n=-\infty}^{\infty} p_\alpha^n(r,z)e^{in\phi}. \tag{11c}$$

Substituting Eqs. (11) into the linearized momentum equations (Eqs.(10)) and the continuity equation (Eq.(7a)), and realizing that for linear analysis only the fundamental components are relevant, we obtain

$$(1-\tau_\theta^2)u_\alpha = \frac{\mathrm{i}}{r}\tau_\theta p_\alpha + \mathrm{i}\frac{\partial p_\alpha}{\partial r} + \mathrm{i}(1+\tau_\theta)z, \tag{12a}$$

$$(1-\tau_\theta^2)v_\alpha = -\frac{1}{r}p_\alpha - \tau_\theta\frac{\partial p_\alpha}{\partial r} - (1+\tau_\theta)z, \tag{12b}$$

$$w_\alpha = \mathrm{i}\frac{\partial p_\alpha}{\partial z}, \tag{12c}$$

$$\frac{\partial^2 p_\alpha}{\partial r^2} + \frac{1}{r}\frac{\partial p_\alpha}{\partial r} - \frac{p_\alpha}{r^2} + (1-\tau_\theta^2)\frac{\partial^2 p_\alpha}{\partial z^2} = 0, \tag{12d}$$

where

$(u_\alpha^1, v_\alpha^1, w_\alpha^1, p_\alpha^1) = \varepsilon(u_\alpha, v_\alpha, w_\alpha, p_\alpha)$ and $\tau_\theta = 2(1+\tau_z)$. The boundary conditions associated with the pressure equations (Eqs.(12d)) at the end walls ($z = \pm\eta$) follow from Eqs. (12c), and they are

$$\frac{\partial p_0}{\partial z} = \frac{\partial p_1}{\partial z} = 0 \quad \text{at} \quad z = \pm\eta. \tag{13}$$

While the boundary condition at the side wall ($r=1$) is found from Eqs. (12a),

$$\frac{\tau_\theta}{r}p_1 + \frac{\partial p_1}{\partial r} = -(1+\tau_\theta)z \quad \text{at} \quad r = 1, \tag{14}$$

and the conditions at the interface are

$$\frac{\tau_\theta}{r}p_0 + \frac{\partial p_0}{\partial r} - \frac{\tau_\theta}{r}p_1 - \frac{\partial p_1}{\partial r} = 0 \quad \text{at} \quad r = r_0, \tag{15a}$$

and

$$\left\{\begin{array}{l}\left[\rho_0(1-\tau_\theta^2) + \dfrac{\tau_\theta^2}{4}(\rho_0-\rho_1)\right]\dfrac{p_0}{r} + \\ \dfrac{\tau_\theta^2}{4}(\rho_0-\rho_1)\dfrac{\partial p_0}{\partial r} - (1-\tau_\theta^2)\rho_1\dfrac{p_1}{r}\end{array}\right\} = \left(\frac{1}{2} + \frac{\tau_\theta}{4} - \frac{\tau_\theta^2}{4}\right)(\rho_0-\rho_1)z \tag{15b}$$

at $r = r_0$.

The pressure equations (Eqs. (12d)) are elliptic, homogeneous, and possess homogeneous boundary conditions in the axial direction. By means of separation of variables, it can be shown that they support solutions in the form of products of sine waves in z and Bessel functions J_1 and Y_1 in r. Hence, their general solutions can be written as

$$p_\alpha = \sum_{k=0}^{\infty}\left[A_k^\alpha J_1(\beta_k r) + B_k^\alpha Y_1(\beta_k r)\right]\sin(\gamma_k z), \tag{16a}$$

where

$$\gamma_k = (2k+1)\frac{\pi}{2\eta}, \quad \beta_k = \gamma_k\sqrt{\tau_\theta^2 - 1}. \tag{16b}$$

The expansion coefficients B_k^0 must all be zero for the inner solution p_0 to be finite as $r \to 0$. However, the expansion coefficients A_k^0, A_k^1, and B_k^1 are determined by satisfying the boundary conditions at the side walls (14) and at the interface (15). Most importantly, they provide us with a criterion for the onset of resonance.

CRITERION FOR RESONANCE

The no-penetration condition at the side wall requires

$$\sum_{k=0}^{\infty}\left\{\begin{matrix}A_k^1[E_1 J_0(\beta_k) + E_2 J_2(\beta_k)] \\ +B_k^1[E_1 Y_0(\beta_k) + E_2 Y_2(\beta_k)]\end{matrix}\right\}\frac{\beta_k}{2}\sin(\gamma_k z) = -E_1 z, \tag{17a}$$

where $E_1 = (1+\tau_\theta)$, $E_2 = (\tau_\theta - 1)$, and J_0, J_2, Y_0, and Y_2 are Bessel functions. While the condition of continuity of the pressure across the interface gives

$$\sum_{k=0}^{\infty}\left\{\begin{matrix}A_k^0[E_6 J_0(\beta_k r_0) + E_7 J_2(\beta_k r_0)] \\ -A_k^1 E_0[J_0(\beta_k r_0) - J_2(\beta_k r_0)] \\ -B_k^1 E_0[Y_0(\beta_k r_0) - Y_2(\beta_k r_0)]\end{matrix}\right\}\frac{\beta_k}{2}\sin(\gamma_k z) = E_5 z, \tag{17b}$$

where

$$E_0 = (1-\tau_\theta^2)\rho_1,\ E_5 = -(\frac{1}{2}+\frac{\tau_\theta}{2}-\tau_\theta^2)(\rho_0-\rho_1),$$

$$E_6 = (1-\tau_\theta^2)\rho_0 + \frac{1}{4}(\tau_\theta^2+\tau_\theta^3)(\rho_0-\rho_1),$$

$$E_7 = (1-\tau_\theta^2)\rho_0 + \frac{1}{4}(\tau_\theta^3-\tau_\theta^2)(\rho_0-\rho_1),$$

and the condition of continuity of radial velocity across the interface provides

$$\sum_{k=0}^{\infty}\begin{Bmatrix} A_k^0[E_1J_0(\beta_k r_0)+E_2J_2(\beta_k r_0)] \\ -A_k^1[E_1J_0(\beta_k r_0)+E_2J_2(\beta_k r_0)] \\ -B_k^1[E_1Y_0(\beta_k r_0)+E_2Y_2(\beta_k r_0)] \end{Bmatrix}\frac{\beta_k}{2}\sin(\gamma_k z) = 0. \qquad (17c)$$

Thus, A_k^0, A_k^1, and B_k^1 are related by

$$\begin{Bmatrix} A_k^1[E_1J_0(\beta_k)+E_2J_2(\beta_k)] \\ +B_k^1[E_1Y_0(\beta_k)+E_2Y_2(\beta_k)] \end{Bmatrix} = \frac{4E_1(-1)^{k+1}}{\eta\gamma_k^2\beta_k}, \qquad (18a)$$

$$\begin{Bmatrix} A_k^0[E_6J_0(\beta_k r_0)+E_7J_2(\beta_k r_0)] \\ -A_k^1E_0[J_0(\beta_k r_0)-J_2(\beta_k r_0)] \\ -B_k^1E_0[Y_0(\beta_k r_0)-Y_2(\beta_k r_0)] \end{Bmatrix} = \frac{4E_5(-1)^{k+1}}{\eta\gamma_k^2\beta_k}, \qquad (18b)$$

$$\begin{Bmatrix} A_k^0[E_1J_0(\beta_k r_0)+E_2J_2(\beta_k r_0)] \\ -A_k^1[E_1J_0(\beta_k r_0)+E_2J_2(\beta_k r_0)] \\ -B_k^1[E_1Y_0(\beta_k r_0)+E_2Y_2(\beta_k r_0)] \end{Bmatrix} = 0. \qquad (18c)$$

Consequently the motion becomes resonant if the determinant of the above system vanishes,

$$[E_1 J_0(\beta_k) + E_2 J_2(\beta_k)][E_1 Y_0(\beta_k r_0) + E_2 Y_2(\beta_k r_0)][E_6 J_0(\beta_k r_0) + E_7 J_2(\beta_k r_0)]$$
$$-[E_1 J_0(\beta_k) + E_2 J_2(\beta_k)][E_0 J_0(\beta_k r_0) - E_0 J_2(\beta_k r_0)][E_1 J_0(\beta_k r_0) + E_2 J_2(\beta_k r_0)]$$
$$-[E_1 Y_0(\beta_k) + E_2 Y_2(\beta_k)][E_1 J_0(\beta_k r_0) + E_2 J_2(\beta_k r_0)][E_8 J_0(\beta_k r_0) + E_9 J_2(\beta_k r_0)]$$
$$= 0, \qquad (19)$$

where

$$E_8 = E_6 - E_0, \text{ and } E_9 = E_7 + E_0.$$

This equation is quite complicated since it depends on τ, θ, η, k,and ρ_0/ρ_1. Given τ, θ, ρ_0/ρ_1, and k, the solution to equation (19) provides the pairs (r_0, η) that lead to resonance. These pairs constitute continuous functions $\eta = \eta(r_0)$, and for a given interval, $\eta_{min} \le \eta \le \eta_{max}$, there may be more than one function and the number of functions increases with k. Plots of these functions are shown in figures 2 through 7 for k = 0, 1, 2, 3, 4, and 5 respectively.

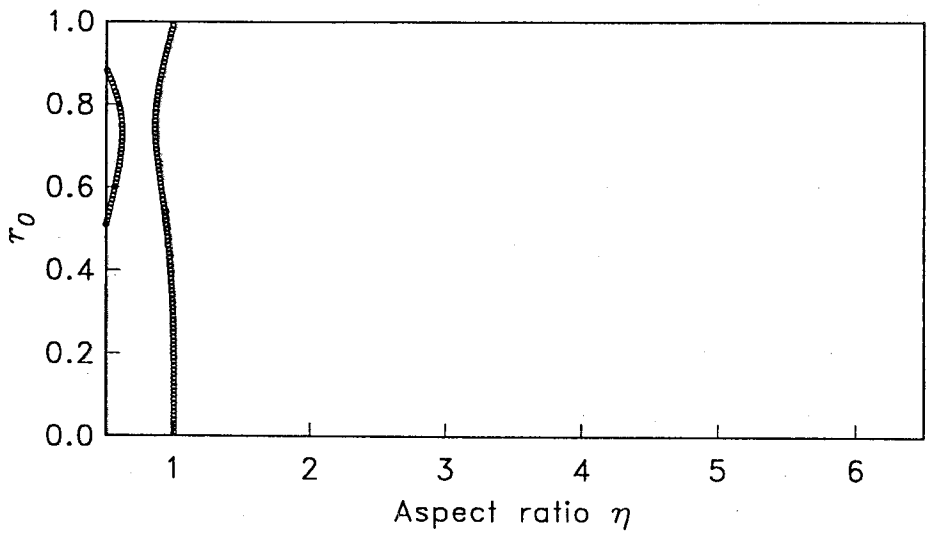

Figure 2: **Plot of the roots of Eq. (19) for k = 0, τ = 0.008, θ = 1°, and ρ_0/ρ_1 = 0.2.**

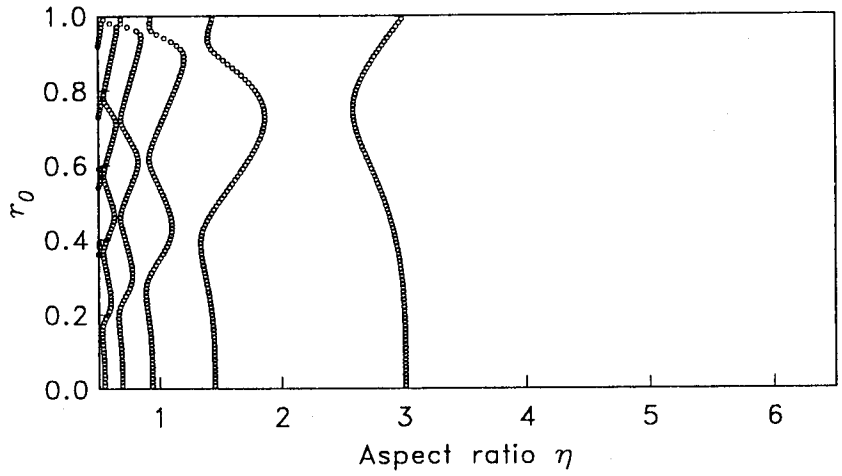

Figure 3: **Plot of the roots of Eq. (19) for k = 1, $\tau = 0.008$, $\theta = 1^o$, and $\rho_0/\rho_1 = 0.2$.**

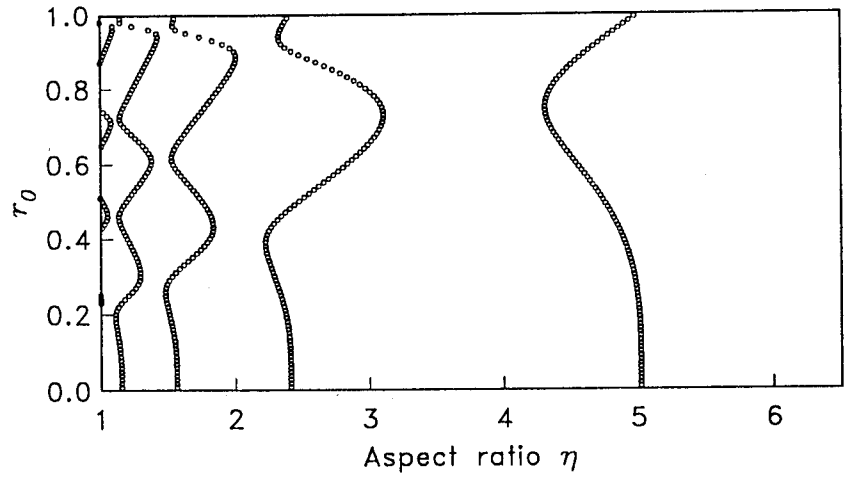

Figure 4: **Plot of the roots of Eq. (19) for k = 2, $\tau = 0.008$, $\theta = 1^o$, and $\rho_0/\rho_1 = 0.2$.**

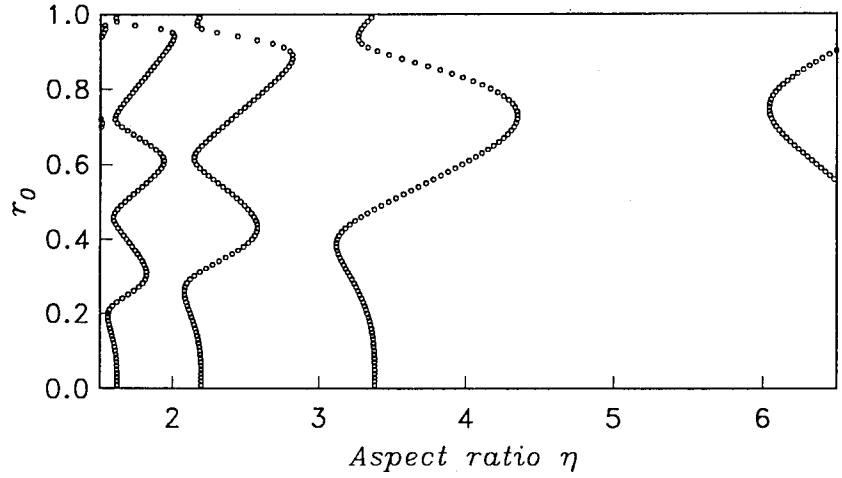

Figure 5: **Plot of the roots of Eq. (19) for k = 3, τ = 0.008, θ = 1°, and ρ_0/ρ_1 = 0.2.**

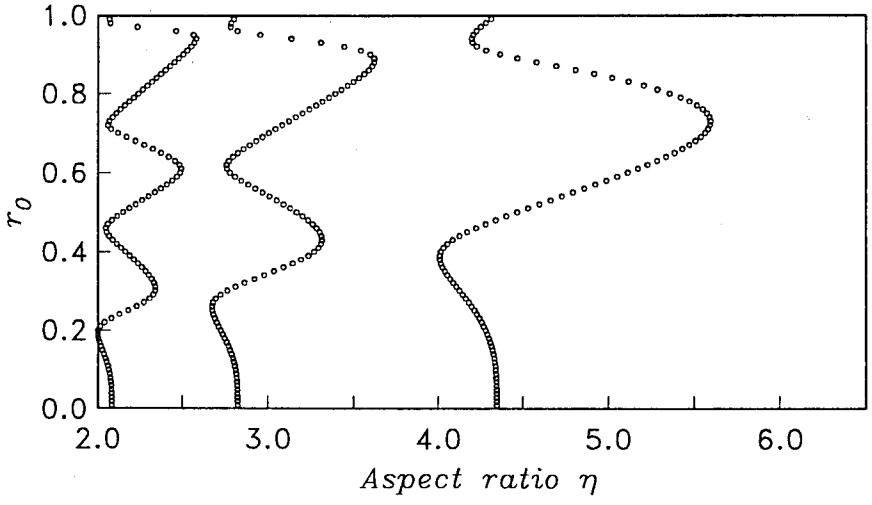

Figure 6: **Plot of the roots of Eq. (19) for k = 4, τ = 0.008, θ = 1°, and ρ_0/ρ_1 = 0.2.**

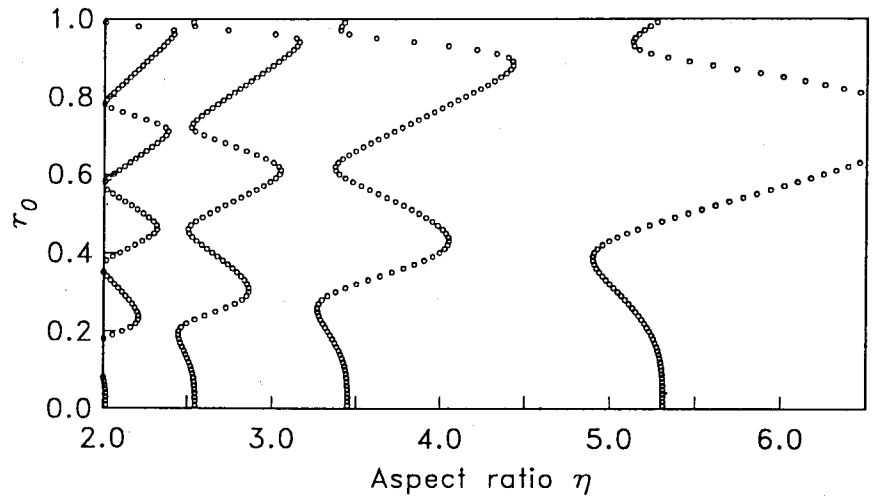

Figure 7: Plot of the roots of Eq. (19) for k = 5, τ = 0.008, θ = 1°, and ρ_0/ρ_1 = 0.2.

If we plot the same results in one figure, it would be filled with small circles indicating resonance of some value k. However, not every critical pair (r_0, η) leads to the most amplifications in the roll moment. For a given region in the $r_0 - \eta$ plane some are more critical than others. We could choose to plot the critical values associated with the lowest values of k as in figure 8 or plot only the critical values leading to the most amplification in the moments as in figure 9. We prefer the latter approach, and we obtained plots or diagrams of this sort for different values of the density ratio. Some of these results are shown in figures 10 and 11. We note from these figures that as $\rho_0 \to \rho_1$ we retrieve the results for a cylinder completely filled with a single fluid (Selmi *et al.* 1992). However, some critical values become degenerate since they would cancel out with terms in the numerators of the expansion coefficients in the limit as $\rho_0 \to \rho_1$. Degenerate modes are also found in the limit as $r_0 \to 0$ and as $\rho_0/\rho_1 \to 0$. In this latter case, some of the most critical values approach those for partially filled cylinders (Selmi & Herbert 1992), while others are degenerate. We recommend that the appropriate equations for the limiting configuration be used to compute the critical values.

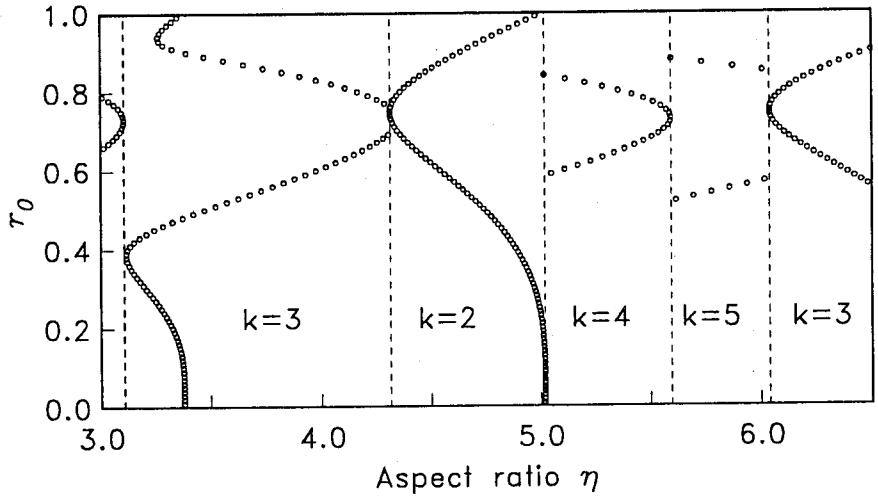

Figure 8: **Plot of the most critical roots of Eq. (19) for $\tau = 0.008$, $\theta = 1^0$, and $\rho_0/\rho_1 = 0.2$.**

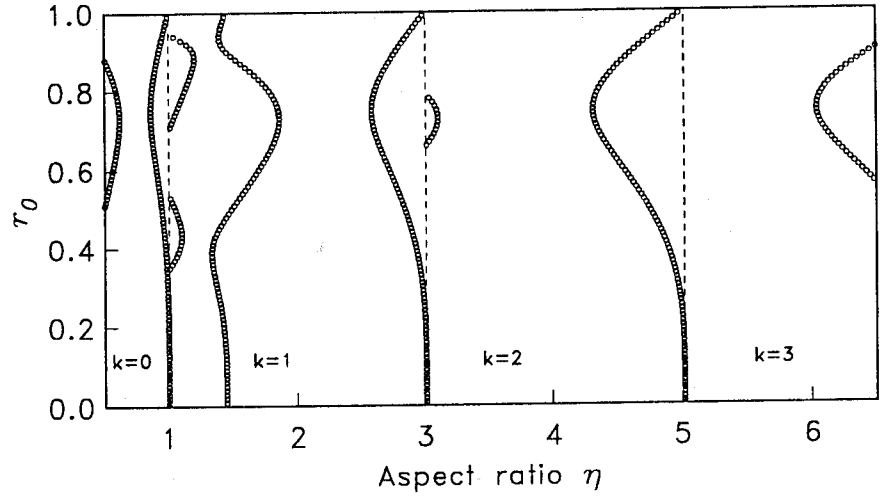

Figure 9: **Dimensionless fill radius versus aspect ratio causing primary (most dangerous) resonance in cylinders containing two immiscible fluids at $\tau = 0.008$, $\theta = 1^0$, and $\rho_0/\rho_1 = 0.2$.**

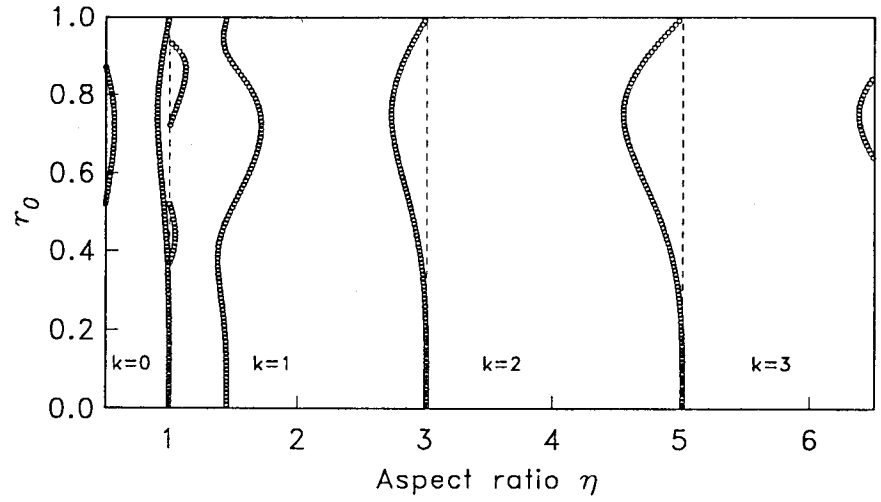

Figure 10: **Dimensionless fill radius versus aspect ratio causing primary (most dangerous) resonance in cylinders containing two immiscible fluids at $\tau = 0.008$, $\theta = 1^{o}$, and $\rho_0/\rho_1 = 0.4$.**

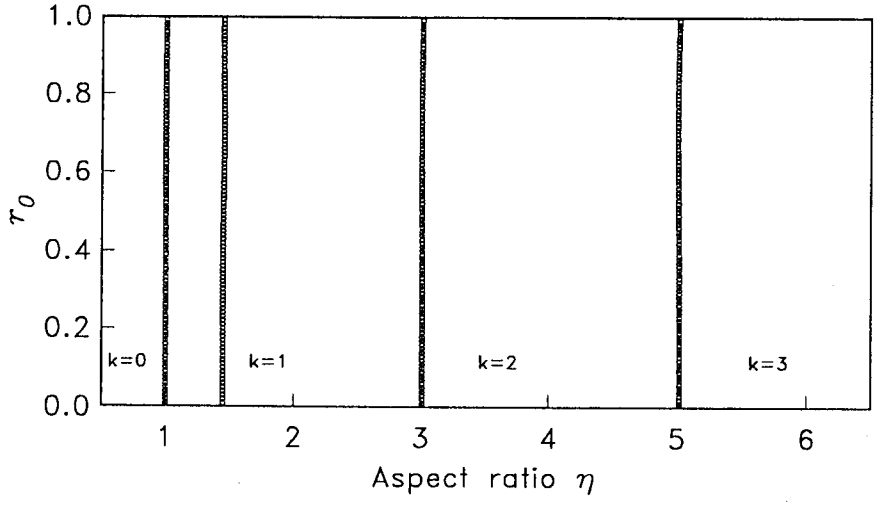

Figure 11: **Dimensionless fill radius versus aspect ratio causing primary (most dangerous) resonance in cylinders containing two immiscible fluids at $\tau = 0.008$, $\theta = 1^{o}$, and $\rho_0/\rho_1 = 0.98$.**

In figures 12 and 13 we show comparisons of our results with those obtained by Selmi (1991) and Selmi *et al.* (1993) for two viscous fluids. Figure 12 shows plots of the dimensionless roll moment versus the dimensionless fill radius for different inner-fluid Reynolds number $Re_0 = \omega a^2/\nu_0$ and outer-fluid Reynolds number $Re_1 = \omega a^2/\nu_1$, where ν_0 and ν_1 denote the kinematic viscosity of inner and outer fluid respectively. Figure 13 shows similar plots for the dimensionless yaw moment versus the dimensionless fill radius. In both figure 12 and figure 13 the inviscid results are shown by vertical dashed lines indicating the critical dimensionless fill radii at which resonance occur. We see clearly that as the Reynolds numbers increase, the critical dimensionless fill radii given by the viscous analysis approach those given by the inviscid analysis presented in this paper.

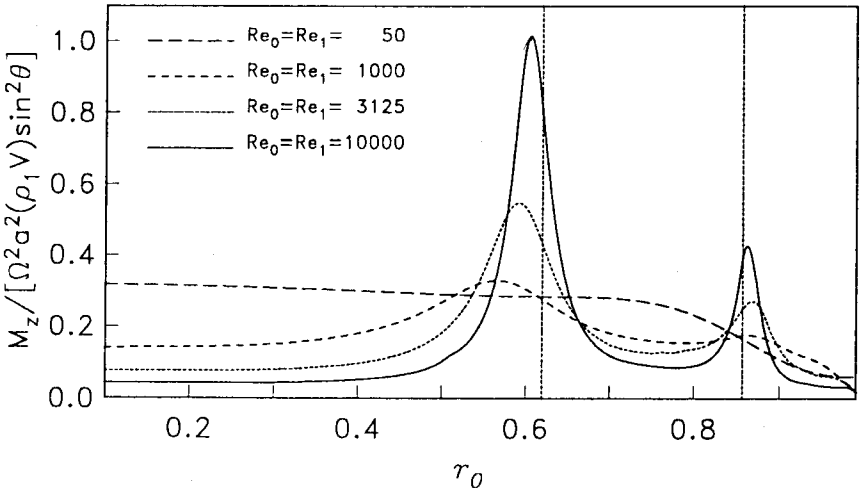

Figure 12: **Dimensionless roll moment versus dimensionless fill radius for cylinders containing two immiscible fluids at $\tau = 0.008$, $\theta = 1^0$, and $\rho_0/\rho_1 = 0.2$. Comparison of the inviscid results (vertical dashed lines) and the viscous results of Selmi (1991).**

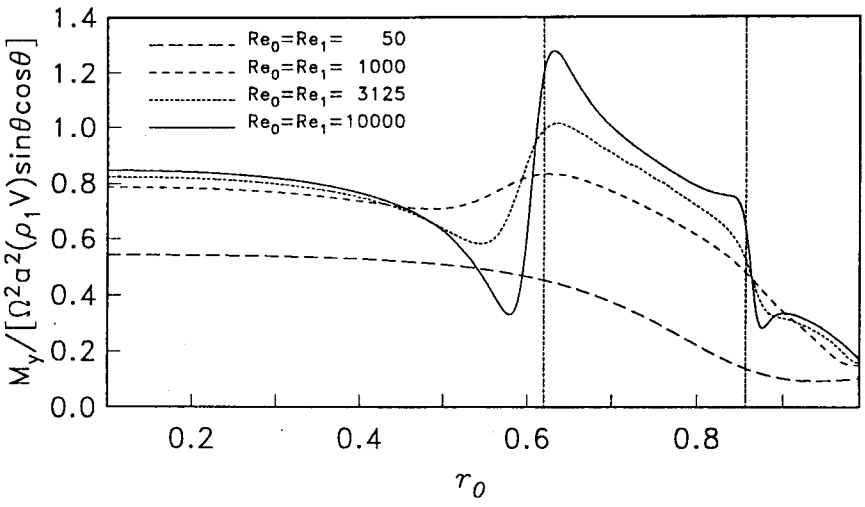

Figure 13: **Dimensionless pitch moment versus dimensionless fill radius for cylinders containing two immiscible fluids at $\tau = 0.008$, $\theta = 1^0$, and ρ_0/ρ_1**

SUMMARY

We have presented a method for solving the equations governing two inviscid fluids inside a spinning and coning cylinder for small coning angles and/or coning frequencies. The equations governing the fundamental components of the velocity and pressure in each region were reduced to a second order equation governing the pressure. The two equations governing the pressure in both inner and outer regions have homogenous boundary conditions at the end walls. This enabled us to use separation of variables to solve both equations analytically. Satisfying the no-penetration conditions at the side wall and the continuity of pressure across the interface provided a criterion in the form of a transcendental equation that can be solved numerically for the parameters that cause resonance. We have presented some of these parameters by solving the transcendental equation by Newton-Raphson's method.

ACKNOWLEDGMENTS

The author greatly acknowledges the open discussion with Dr. Rihua Li, Professor Thorwald Herbert, and Miles C. Miller. Part of the calculations was performed on the Cray Y-MP8/864 of the Ohio Supercomputer Center while the author was at Ohio State University.

REFERENCES

1. **Hall, P., Sedney, R. and Gerber, N. 1990.** Dynamics of the fluid in a spinning coning cylinder, AIAA Journal, Vol. 28, No 5, pp. 828-835.

2. **Murphy, C. M. 1985.** A relation between liquid roll moment and liquid side moment, J. Guidance, Control, Dynamics 8, 287-288.

3. **Herbert, Th. 1985.** Viscous fluid motion in a spinning and nutating cylinder, J. Fluid Mech. 167, pp. 181-198.

4. **Herbert, Th. and Li, R. 1990.** Computational study of the flow in a spinning and nutating cylinder, AIAA Journal Vol 28, No. 9, pp. 1596-1604.

5. **Miller, M. C. 1991.** Elimination of viscous liquid-fill instability by means of lower viscosity, immiscible liquid additive, AIAA Paper No. 91-0679.

6. **Selmi, M. 1991.** Resonance phenomena in viscous fluid configurations inside a spinning and coning cylinder, Ph.D. Dissertation, The Ohio State University, Columbus, Ohio U.S.A.

7. **Selmi, M. and Herbert, Th. 1992.** Resonance Phenomena in partially filled spinning and nutating cylinders, submitted to Physics of Fluids A..

8. **Selmi, M., Li, R. and Herbert, Th. 1992.** Dynamics of two-immiscible fluids in a spinning and nutating cylinder, in preparation for Physics of Fluids A.

9. **Selmi, M., Li, R. and Herbert, Th. 1992.** Eigenfunction expansion of the flow in a spinning and nutating cylinder, Physics of Fluids A, Vol. 4 No. 9, 1992.

10. **Stewartson, K 1959.** On the stability of a spinning top containing liquid, J. Fluid Mech. 5,(4), 577-592.

11. **Wedemeyer, E. H. 1966.** Viscous corrections to Stewartson's stability criterion, Ballistic Research Laboratory Report 1325.